he Numerical Solution of ree Surface/Pressurized low in Pipes

Ian MacDonald

September 1992

Submitted to the

Department of Mathematics,

University of Reading,

in partial fulfillment of the requirements for the

Degree of Master of Science

Flows in closed channels can change from free surface flow to pressurized flow and

Contents

In a closed channel (pipe, channel with soffit) there are often situations which involve a transition from free surface flow to pressurized flow, or vice versa. For example if we have a closed channel in a hydraulic plant, with initially free surface flow, then the start-up of machinery (pumps, turbines) may cause a steep wave for conservation laws. Traditional schemes, such as Lax Wendroff and central difference, are unsplit (that is they take no account of the direction of flow). These schemes often inherently cause oscillations in space, near discontinuities. Since the 1980's, upwind schemes have become popular, since they are found to give better results for conservation laws, the main examples of these being Roe, Osher and Van Leer.

Roe's scheme has been tried in [1] for this problem, but the scheme is observed to give oscillations in time. In this work we investigate the cause of these oscillations, and attempt to alleviate the problem.

In chapter 2 we quote and describe the open channel equations, justify the use of the slot and set up the problem that forms the basis of this work.

The first thing we do after reproducing the results in [1], is to try some other upwind schemes in order to see what effect they have on the oscillations. This forms chapters 3 to 5.

The presence of the narrow slot causes a sharp jump in the characteristic waves speeds as we enter the slot. In chapter 6 we try two different ways of smoothing this jump to see what effect this has on the oscillations.

In chapter 7 we try an implicit version of Roe's scheme, and also alternatives to uler time stepping.

In chapter 8 we develop a 'shock' fitting modification to Roe's scheme.

In chapter 9 we summarise the conclusions we have made from the proceeding chapters.

Ch pter 2

Simul tion of ressurized Flow with the Open Ch nnel E u tions

2.1 The Open hannel Equations

The unsteady 1-D open channel equations, often referred to as the St. Venant equations, can, for a prismatic channel (i.e. constant cross-section), be written in conservation form as follows (see [12] pp. 451 or [2] pp. 7, for the derivation),

$$\frac{\partial \mathbf{w}}{\partial t} + \frac{\partial \mathbf{F}(\mathbf{w})}{\partial x} = \mathbf{D} \tag{2.1}$$

where

$$\mathbf{w} = \begin{bmatrix} A \\ Q \end{bmatrix}, \ \mathbf{F}(\mathbf{w}) = \begin{bmatrix} Q \\ \dfrac{Q^2}{A} + I_1(A) \end{bmatrix}, \ \mathbf{D} = \begin{bmatrix} 0 \\ gA(S_0 - S_f) \end{bmatrix}.$$

quation (2.1) uses the following notation

h = water depth

0

f

h

1 0

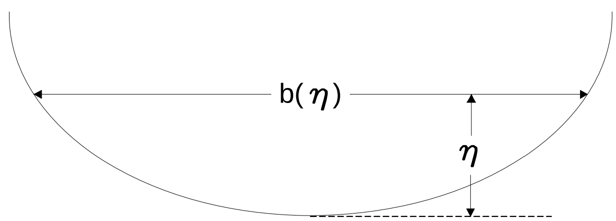

2

4 3

$$\rho \quad = \quad \text{density}$$

The friction slope S_f is defined by

$$S_f = \frac{1}{\rho g A} F_f$$

hence

$$S_f = \frac{v\ v}{R^{4/3}} \quad \frac{n}{1.49} \quad ^2 \tag{2.2}$$

We can write equation (2.1) as

$$\frac{\partial}{\partial t} + J(\quad)\frac{\partial}{\partial x} =$$

where J is the Jacobian of

$$J(\quad) = \frac{\partial \ (\quad)}{\partial} = \begin{matrix} 0 & 1 \\ \frac{Q^2}{A^2} + c^2 & \frac{2Q}{A} \end{matrix}$$

where

$$c^2 = \frac{d}{dA} I_1(A).$$

If $b(\eta)$ is continuous at $\eta = h$, then

$$\begin{aligned} c^2 = \frac{d}{dA} \int_0^h g(h \quad \eta) b(\eta) d\eta &= \quad \frac{dh}{dA} \frac{d}{dh} \int_0^h g(h \quad \eta) b(\eta) d\eta \quad h \quad a \ m \ g \ k \quad d \quad h \quad f \quad h \\ &= \quad \text{—} \quad \int_0^h (\ ) \quad + \ (\qquad) \ (\ ) \\ &= \qquad\qquad \text{—} \int_0^h (\ ) \end{aligned}$$

From the definition of wetted area, we know that

$$= \int_0^h (\ )$$

so

$$\text{—} = (\ ) = \ _s$$

where $_s$ is the channel width at the free surface; hence we have that

$$^2 = \frac{}{_s} \tag{2 3}$$

$_1$ — $_2$ —

1 **2**

1 2

sl

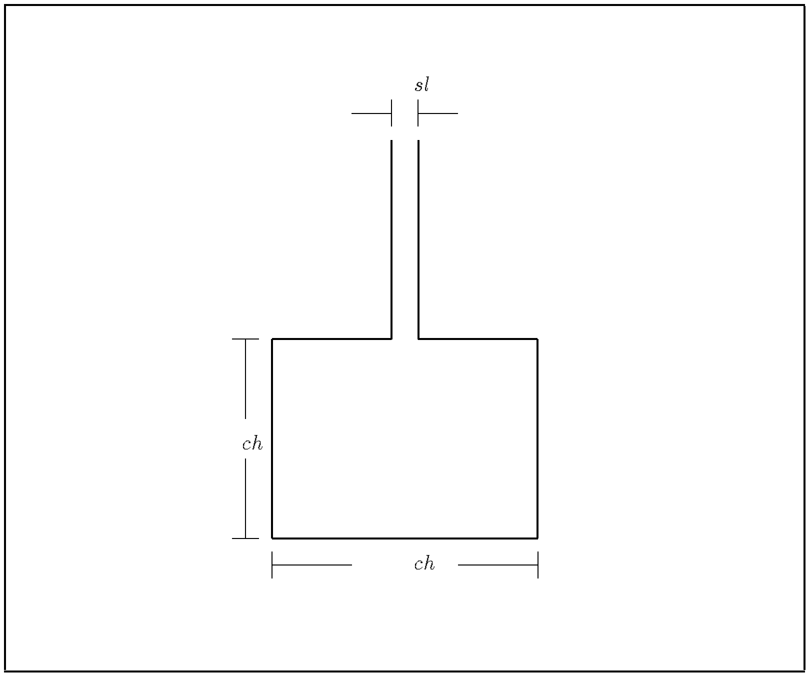
sl
ch
ch

2.3 Description of the Problem

The problem tackled in this work is from [1]. It consists of a rectangular channel, as in figure 2.2. The properties of the channel are given as follows,

$$
\begin{aligned}
\text{Channel width } (w_{ch}) &= 0.51\text{m} \\
\text{Channel height}(h_{ch}) &= 0.148\text{m} \\
\text{Channel length} &= 10\text{m} \\
\text{Channel slope} &= 0 \\
\text{Manning constant}(n) &= 0.012 \\
\text{Slot width}(w_{sl}) &= 0.01\text{m.}
\end{aligned}
$$

The following initial conditions are given

$$
\begin{aligned}
A(x,0) &= 0.06528 \text{ m}^2 \\
Q(x,0) &= 0 \text{ m}^3\text{s}^{-1}.
\end{aligned}
$$

The boundary conditions are given by the following data

At $x = 0$ (see figure 2.3)

Time (s)	Water depth (m)	Time (s)	Water depth (m)
0.0	0.1280	3.4	0.1728
0.2	0.1290	3.6	0.1752
0.4	0.1300	3.8	0.1778
0.6	0.1330	4.0	0.1800
0.8	0.1360	4.2	0.1830
1.0	0.1400	4.4	0.1870
1.2	0.1420	4.6	0.1900
1.4	0.1440	4.8	0.1920
1.6	0.1460	5.0	0.1920
1.8	0.1470	5.2	0.1916
2.0	0.1500	5.4	0.1896
2.2	0.1516	5.6	0.1880
2.4	0.1540	5.8	0.1880
2.6	0.1580	6.0	0.1888
2.8	0.1610	6.2	0.1908
3.0	0.1640	6.4	0.1948
3.2	0.1688	6.6	0.1972

At = 10 0

Time (s)	Water depth (m)	Time (s)	Water depth (m)
0 0	0 1280	6 6	0 1280

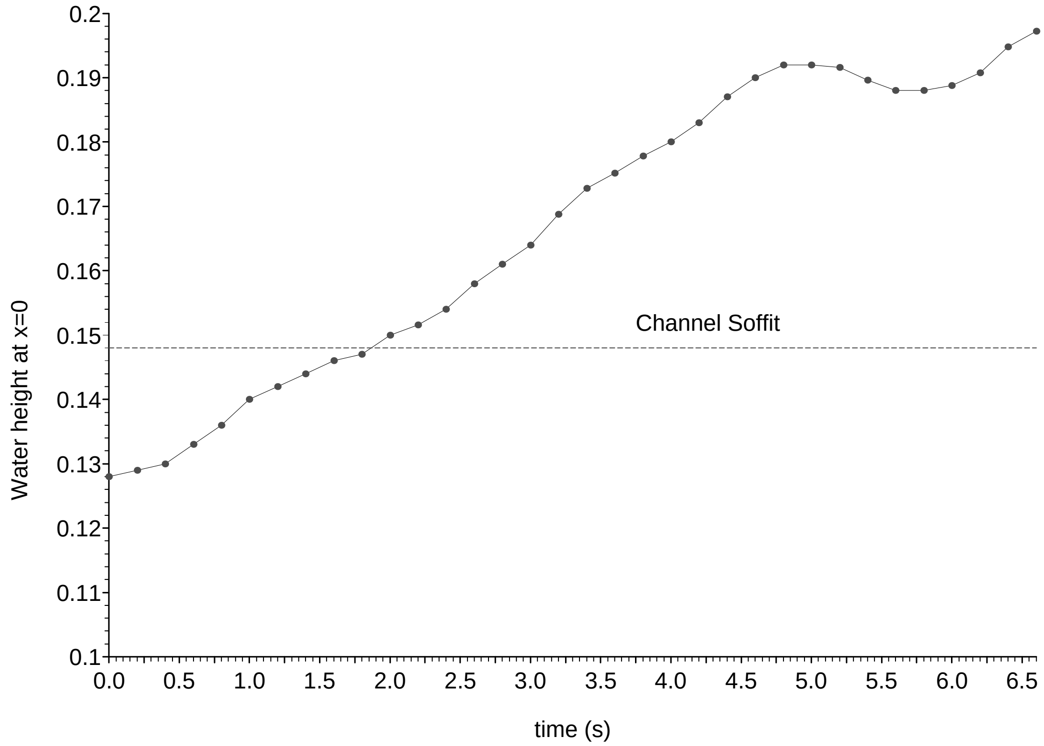

The main thing that we need to calculate for our problem, is the integral $I_1(A)$ (see equation (2.1)). This is given by the following formula

$$I_1(A) = \begin{cases} \dfrac{gA^2}{2w_{ch}} & A \leq A_{crit} \\ gA_{crit}\left(\dfrac{(A-A_{crit})}{w_{sl}} + \dfrac{h_{ch}}{2}\right) + \dfrac{g(A-A_{crit})^2}{2w_{sl}} & A > A_{crit} \end{cases}$$

where $A_{crit} = h_{ch}w_{ch}$.

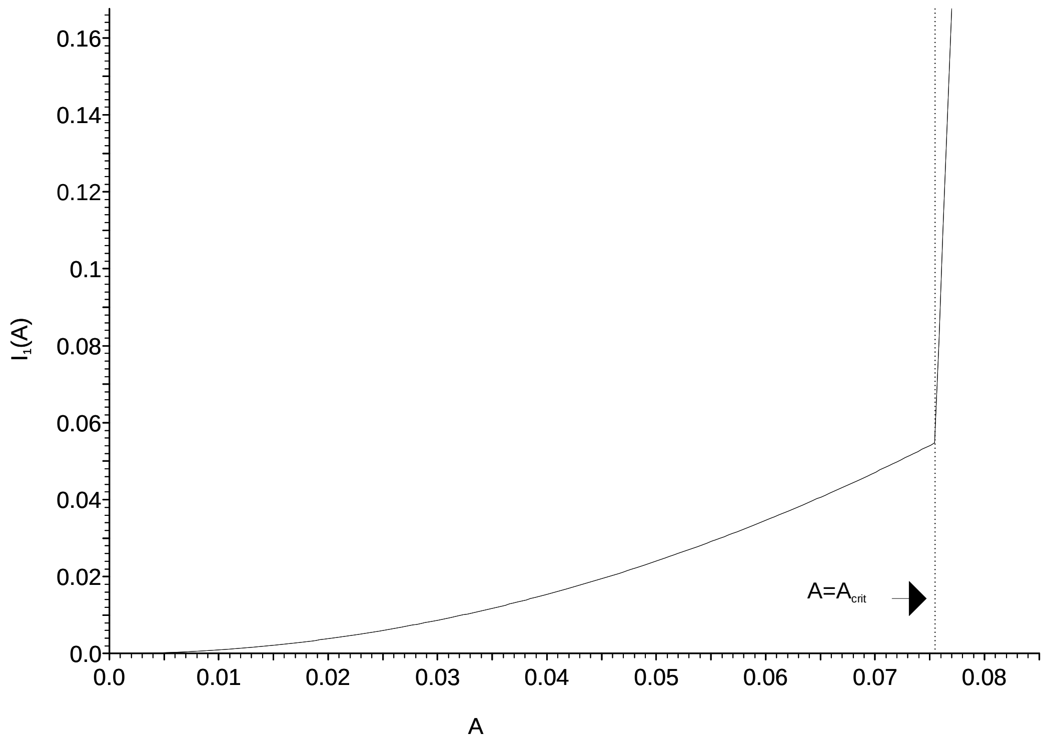

Figure 2.4: Plot of $I_1(A)$ for our channel.

I_1 (see figure 2.4) is a continuous function, and it is differentiable everywhere, except at $A = A_{crit}$. c is not strictly defined at this point, although we can take limits from above and below,

$$c_- = \left(\frac{gA_{crit}}{w_{ch}}\right)^{1/2}, \qquad c_+ = \left(\frac{gA_{crit}}{w_{sl}}\right)^{1/2}.$$

c (see figure 2.5) is then discontinuous at $A = A_{crit}$, and the jump is given by

$$\Delta c = c_+ - c_-.$$

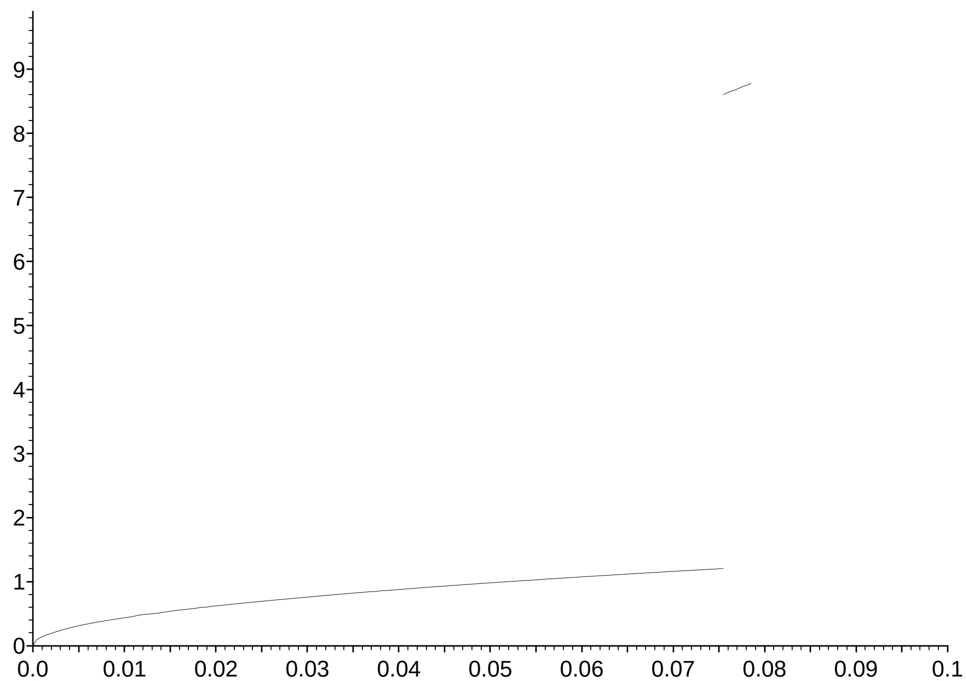

0
1
2
3
4
5
6
7
8
9
0.0
0.01
0.02
0.03
0.04
0.05
0.06
0.07
0.08
0.09
0.1

Ch pter 3

Roe's Scheme

3.1 Description of the Scheme

This scheme was originally developed for the uler equations in [9]. In common with other schemes used in this work, we approximate the solution function $w(x)$, by a set of piecewise constant states $\{w_j\}$, of constant width Δx (see figure 3.1).

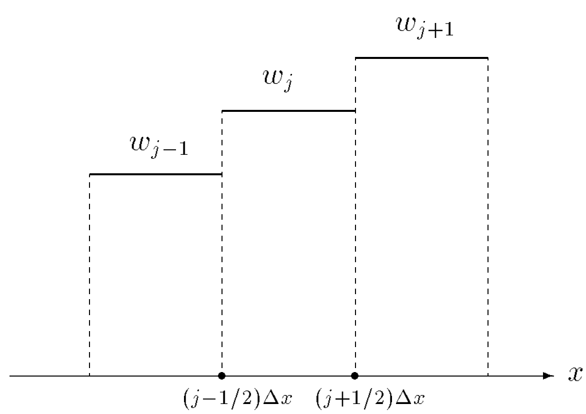

Figure 3.1: Piecewise constant states.

w_j is taken to be the cell average of the function w, on the interval

$$[(j-1/2)\Delta x, (j+1/2)\Delta x]$$

and is given by

$$w_j = \frac{1}{\Delta x} \int_{(j-1/2)\Delta x}^{(j+1/2)\Delta x} w(x) dx$$

This property ensures that the piecewise constant approximation has the 'same amount of w' as the original function.

Suppose $\{\mathbf{w}_j^n\}$ are the cell averages to some approximation of the exact solution of the PD (2.1) with $\mathbf{D} = \mathbf{0}$, at $t = n\Delta t$. We then have a sequence of Riemann problems centred at $x = (j + 1/2)\Delta x, t = n\Delta t$, $j = 0, 1, \ldots$.

In Roe's scheme we approximate the Jacobian, $J(\mathbf{w})$, in the interval $[j\Delta x, (j+1)\Delta x]$ by the constant matrix $\tilde{J}(\mathbf{w}_L, \mathbf{w}_R)$, where $\mathbf{w}_L = \mathbf{w}_j^n$ and $\mathbf{w}_R = \mathbf{w}_{j+1}^n$. We can then solve the Riemann problem exactly, with this new constant matrix (see below).

The matrix $\tilde{J}$ is chosen so to have the following three properties,

1. As $\mathbf{w}_L \rightarrow \mathbf{w}_R \rightarrow \mathbf{w}$

   $\tilde{J}(\mathbf{w}_L, \mathbf{w}_R) \rightarrow J(\mathbf{w})$

2. For any $\mathbf{w}_L, \mathbf{w}_R$

   $\tilde{J}(\mathbf{w}_L, \mathbf{w}_R)(\mathbf{w}_R - \mathbf{w}_L) = \mathbf{F}(\mathbf{w}_R) - \mathbf{F}(\mathbf{w}_L)$

3. The eigenvectors of $\tilde{J}$ are linearly independent.

These three properties ensure conservation, and that any shock will satisfy the Rankine-Hugoniot condition (See [9] for more details).

The matrix that has these properties is as follows,

$$\tilde{J}(\mathbf{w}_L, \mathbf{w}_R) = \begin{bmatrix} 0 & 1 \\ -\dfrac{\tilde{Q}^2}{\tilde{A}^2} + \tilde{c}^2 & \dfrac{2\tilde{Q}}{\tilde{A}} \end{bmatrix}$$

where

$$\tilde{\ } = (\ _L \ _R)^{1/2}$$

$$\tilde{\ } = \frac{(\ _L)^{1/2} \ _R + (\ _R)^{1/2} \ _L}{(\ _L)^{1/2} + (\ _R)^{1/2}}$$

$$\tilde{\ } = \begin{cases} \left(\frac{ _1(\ _R) \quad _1(\ _L)}{ \ _R \quad \ _L}\right)^{1/2} & \ _R \quad \ _L = 0 \\ \left(\frac{(\ _R + \ _L)}{(\ _s)_R + (\ _s)_L}\right)^{1/2} & \ _R \quad \ _L = 0 \end{cases}$$

$\tilde{\ }$ has eigenvalues

$$\tilde{\ }_1 = \frac{\tilde{\ }}{\tilde{\ }} \quad \tilde{\ }, \quad \tilde{\ }_2 = \frac{\tilde{\ }}{\tilde{\ }} + \tilde{\ }$$

and corresponding eigenvectors

$$\mathbf{ _1} = \begin{pmatrix} 1 \\ \tilde{\ }_1 \end{pmatrix}, \quad \mathbf{ _2} = \begin{pmatrix} 1 \\ \tilde{\ }_2 \end{pmatrix}$$

If we decompose the jumps in as follows (see [9])

$$ _R \quad _L = \tilde{\ }_1 \tilde{\ }_1 + \tilde{\ }_2 \tilde{\ }_2$$

then using the properties of the matrix $\tilde{\ }$ the flux difference is

$$(\ _R) \quad (\ _L) = \tilde{\ }_1 \tilde{\ }_1 \tilde{\ }_1 + \tilde{\ }_2 \tilde{\ }_2 \tilde{\ }_2$$

Here $\tilde{\ }_1$ and $\tilde{\ }_2$ are fo22W+˜'Σ2mngB[=bWprop'BC2W+˜'Σ2mhC2W+˜'Σ2st 3igths2W+˜'Σ2C

$_1$ $_2$

$$ _1 \quad \frac{ _2 \ _R \quad _L \quad _R \quad _L}{ _2 \quad _1}$$

$$ _2 \quad \frac{ _R \quad _L \quad _1 \ _R \quad _L}{ _2 \quad _1}$$

$$ _1 \ _1 \quad _2 \ _2$$

where is some average of $_L$ and $_R$, which are the source terms on the left and right. This work uses $= \frac{1}{2}(\ _L + \ _R)$. If $= [0\ \tilde{}\ ]^T$ then

$$\tilde{}_1 = \frac{\tilde{}}{\tilde{}_2 \quad \tilde{}_1}$$

$$\tilde{}_2 = \quad \tilde{}_1$$

We now get to the main part of the algorithm.

Suppose we have $+1$ constant states altogether, then we will have Riemann problems. For the th Riemann problem centred at $= (\ +1 \ 2)\Delta$ we calculate and keep the following

$$\begin{aligned} \tilde{}_{i,j+1/2} &= \tilde{}_i \\ _{i,j+1/2} &= \frac{\Delta}{\Delta}\tilde{}_i\,\tilde{}_i + \Delta\ \tilde{}_i \quad _i \end{aligned} \qquad = 1\ \ 2$$

The terms $_{i,j+1/2}$ are the time updates to the components of (corresponding to

$_1$ $_2$

$_{i,j+1/2}$ $_{j+1}$ $_{i,j+1/2}$

$_j$ $_{i,j+1/2}$

$_{1,j+1/2}$ $_{2,j+1/2}$ $\overline{\quad}$

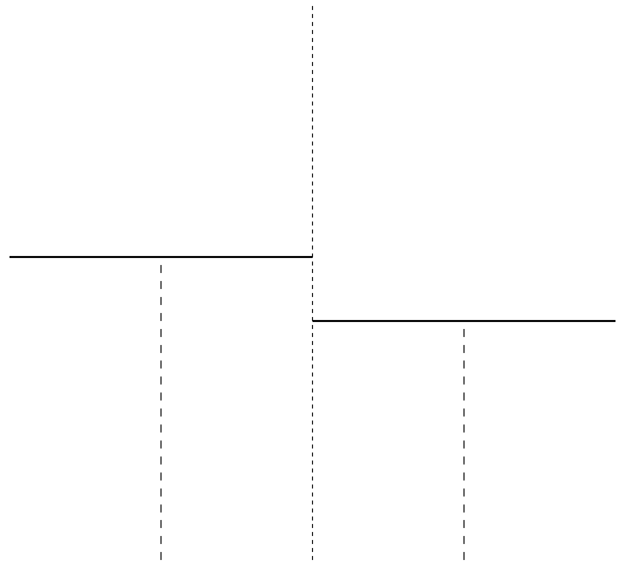

at a boundary, then it is only appropriate to overwrite the incoming characteristic variable, hence we must have only one boundary condition.

The only case encountered in this work is where we have only one incoming wave at each end, and we wish to specify the height of the water at the boundaries for each time step. We can directly overwrite the area variable, A, with the new area (calculated from the new height), but we do not know what to do with the Q variable. This problem can be solved by extrapolating from the interior values near the boundary, an incoming wave at the boundary. The strength of this wave is chosen so as to give the correct value of A at the boundary. This wave is then used to increment the Q value at the boundary. See [3] for details.

In rare situations Roe's scheme can give unphysical solutions, i.e. entropy violating. The solution can have a shock, when the correct entropy satisfying solution has an expansion fan. Aharact4iCOA7Wsho'ohTficaO[TA Whas'BO7A3Whas'BO7O

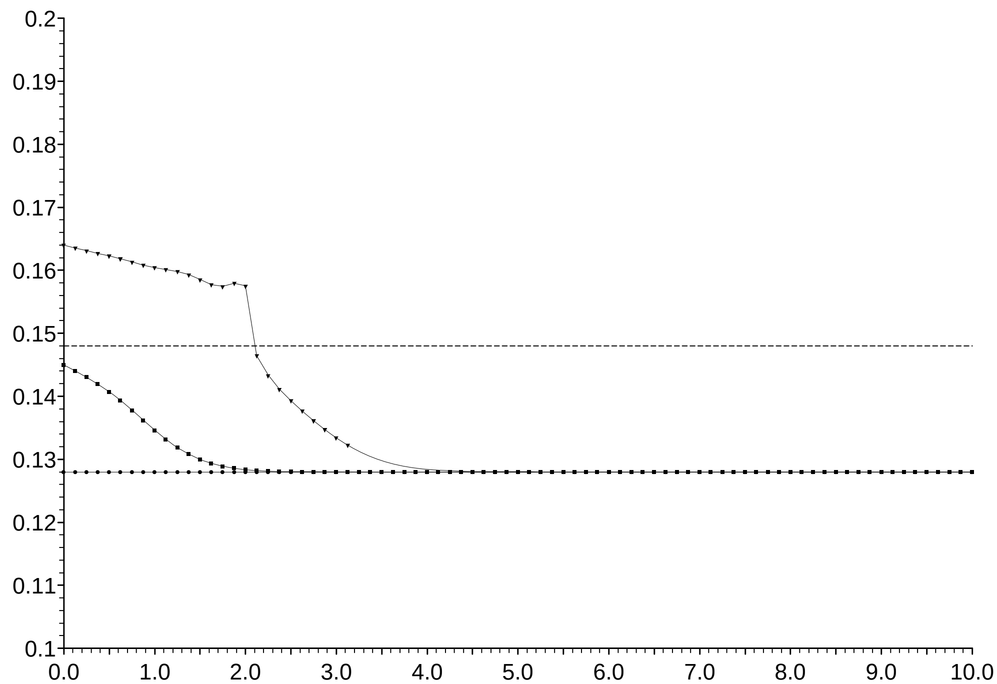

0.2
0.19
0.18
0.17
0.16
0.15
0.14
0.13
0.12
0.11
0.1
0.0
1.0
2.0
3.0
4.0
5.0
6.0
7.0
8.0
9.0
10.0

a series of high frequency oscillations, which eventually decay and the height returns to smooth variation. The oscillations are the ones observed in [1] which prompted this work.

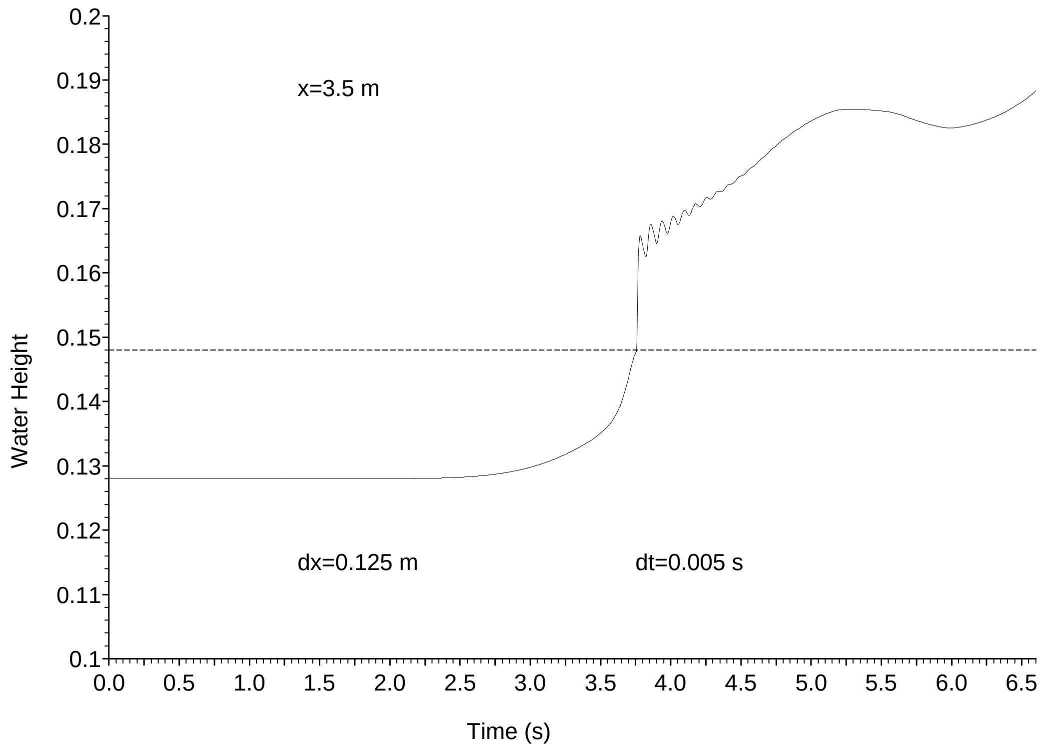

Figure 3.4: Water height against time, at 3.5m along channel.

The most obvious explanation for the oscillations is the discontinuity in the wave celerity, which causes a discontinuity in the characteristic wave speeds (see Figure 2.5). Of course, the scheme cannot resolve this discontinuity, but sees a sharp change in wave speeds as the surface enters the slot. Another problem could be the piece-wise constant approximation, because near the front the solution does not vary smoothly; hence this approximation can become a poor one. The source term could be a cause, but this can practically be ruled out since the oscillations are still present, even for the homogeneous problem.

When the grid is made finer and a smaller time step is used (in order to satisfy

Ch pter

he Osher nd Solomon Scheme

This scheme was used, in order to see if the oscillations observed with Roe's scheme are a peculiarity of Roe's scheme, or whether other schemes suffer from them. See [7] for much more detail on the scheme.

4.1 Description of the Scheme [7]

The Osher and Solomon scheme is the ngquist-Osher scheme generalised to systems. For the scalar conservation law

$$\frac{\partial w}{\partial t} + \frac{\partial f(w)}{\partial x} = 0, \;\; w(x,0) = \phi(x)$$

the ngquist-Osher scheme is as follows

$$w_j^{n+1} = w_j^n - \frac{\Delta t}{\Delta x}(f_-(w_{j+1}^n) - f_-(w_j^n) + f_+(w_j^n) - f_+(w_{j-1}^n))$$

$$w_j^0 = \phi(j\Delta x)$$

Here

$$f_+(u) = \qquad \int_0^u \chi(s) f'(s) ds$$

$$f_-(u) = \int_0^u (1-\chi(s))f'(s)ds$$

where

$$\chi(u) = 1 \quad \Leftrightarrow \quad f'(u) > 0$$

$$\chi(u) = 0 \quad \Leftrightarrow \quad f'(u) \leq 0.$$

We can also write the scheme as follows

$$w_j^{n+1} = w_j^n - \frac{\Delta t}{\Delta x}\left(\int_{w_{j-1}^n}^{w_j^n} \chi(w)f'(w)dw + \int_{w_j^n}^{w_{j+1}^n}(1-\chi(w))f'(w)dw\right)$$

This can be extended to a system in the following way

$$\mathbf{w}_j^{n+1} = \mathbf{w}_j^n - \frac{\Delta t}{\Delta x}\left(\int_{\mathbf{w}_{j-1}^n}^{\mathbf{w}_j^n} \chi(\mathbf{w})J(\mathbf{w})\mathbf{dw} + \int_{\mathbf{w}_j^n}^{\mathbf{w}_{j+1}^n}(I-\chi(\mathbf{w}))J(\mathbf{w})\mathbf{dw}\right)$$

where J is the Jacobian and χ is some matrix that needs to be chosen. We also need to choose the paths of integration.

Let the eigenvalues of J be denoted by $\lambda_1(\mathbf{w}) < \lambda_2(\mathbf{w}) < \ldots < \lambda_m(\mathbf{w})$ with corresponding eigenvectors $\mathbf{e}_1(\mathbf{w}), \mathbf{e}_2(\mathbf{w}), \ldots, \mathbf{e}_m(\mathbf{w})$. Let $T(\mathbf{w})$ be the matrix whose j^{th} column is $\mathbf{e}_j(\mathbf{w})$, then we have that

$$T^{-1}(\mathbf{w})J(\mathbf{w})T(\mathbf{w}) = \text{diag}\{\lambda_k(\mathbf{w})\}.$$

Defining $\chi(\mathbf{w})$ by

$$\chi(\mathbf{w}) = \frac{1}{2}T(\mathbf{w})\text{diag}\{1 + \text{sign}(\lambda_k(\mathbf{w}))\}T^{-1}(\mathbf{w})$$

we have

$$\begin{aligned} \chi(\mathbf{w})J(\mathbf{w}) &= T(\mathbf{w})\text{diag}\{\max(\lambda_k(\mathbf{w}), 0)\}T^{-1}(\mathbf{w}) &&= J^+(\mathbf{w}) \\ (I-\chi(\mathbf{w}))J(\mathbf{w}) &= T(\mathbf{w})\text{diag}\{\min(\lambda_k(\mathbf{w}), 0)\}T^{-1}(\mathbf{w}) &&= J^-(\mathbf{w}) \end{aligned}$$

If Γ^j is the path connecting $\mathbf{w}_{j-1}$ *to* $\mathbf{w}_j$, then we decompose this curve into m sub-curves

$$\Gamma^j = \bigcup_{k=1}^m \Gamma_k^j.$$

These sub-curves are related to rarefaction or compression wave solutions and are defined by

$$\Gamma_k^j = \quad \frac{{}^{(k)}}{} = \quad {}_k \qquad \text{for either } 0 \quad {}_k^{(j)} \text{ or } 0 \quad {}_k^{(j)}$$

$$ {}^{(k)}(0) = \quad {}^{(k+1)}(\; {}_{k+1}^{(j)})$$

$${}^{(m+1)} \; {}_{m+1}^{(j)} \qquad {}_{j-1} \qquad {}^{(1)} \; {}_1^{(j)} \qquad {}_j$$

$${}_j^{n+1} \qquad {}_j^{n} \quad \text{——} \quad \sum_{k=1}^{m} \quad \Gamma_k^j \quad + \qquad \Gamma_k^{j+1} \quad -$$

th

$${}^{(k-1)} \qquad {}^{(k)} \qquad {}_k^{-} \qquad {}_k^{+}$$

$${}^{(k-1)} \qquad {}_j^{k} \qquad {}_k^{-} \qquad {}_k^{+}$$

$$\Gamma_k^j \; {}^{+}$$

$${}_j^{k} \qquad {}^{(k)} \qquad {}_k^{-} \qquad {}_k^{+}$$

$${}_k^{-} \qquad {}_k^{+}$$

$${}^{(k-1)} \qquad {}^{(k)} \qquad {}_k^{-} \qquad {}_k^{+}$$

$${}^{(k-1)} \qquad {}_j^{k} \qquad {}_k^{-} \qquad {}_k^{+}$$

$$\Gamma_k^j \; {}^{-}$$

$${}_j^{k} \qquad {}^{(k)} \qquad {}_k^{-} \qquad {}_k^{+}$$

$${}_k^{-} \qquad {}_k^{+}$$

${}_k^{+}$ ${}_k$ ${}^{(k)}$ ${}_k^{-}$ ${}_k$ ${}^{(k-1)}$

${}_k^{(j)}$ ${}_k$ ${}^{(k)}$ ${}_k^{(j)}$ ${}_j^{k}$ ${}^{(k)}$ ${}_k^{(j)}$

${}_1^{j}$

1 2 ( )
2

1 2 ( )
2
0 $\dfrac{2\ (\ )_2}{2\ (\ )_2}$ $\dfrac{2\ (\ )_2}{2\ (\ )_2}$

2

2
1

2
1
0 $\dfrac{1}{1}$ $\dfrac{1}{1}$

1 $(\ )_1$ 1 $(\ )_1$

2 1 1

1 2 $\overline{2}$

$\overline{}$ $_k^j$ $_k^{j+1}$

$\overline{}$ $_k^1$

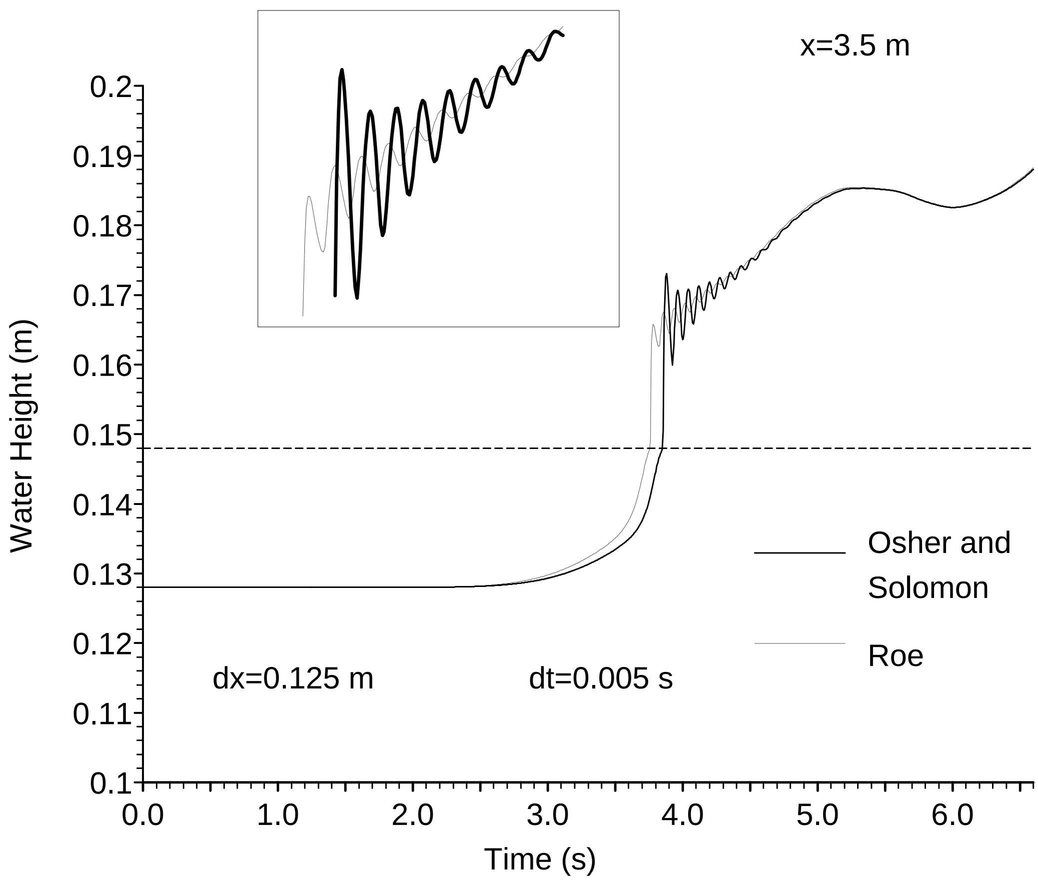

x=3.5 m
Water Height (m)
0.2
0.19
0.18
0.17
0.16
0.15
0.14
0.13
0.12
0.11
0.1
0.0
1.0
2.0
3.0
4.0
5.0
6.0
Time (s)
dx=0.125 m
dt=0.005 s
Osher and Solomon
Roe

After observing that both Roe's scheme and the Osher and Solomon scheme both suffer from the oscillations, the following question must be asked; are the oscillations due to the approximate nature of the Riemann solvers? This was tested by using the exact Riemann solver, i.e. using Godunov's method.

The Riemann problem

$$— + \frac{(\quad)}{\quad} = 0$$

L

R

(R) L R

(see [11]). Let us define the following curves in the (A, Q) plane,

$$\Gamma_1(\mathbf{w}_0) = \{(A,Q); A \geq 0, v + h(A) = v_0 + h(A_0)\}$$

$$\Gamma_2(\mathbf{w}_0) = \{(A,Q); A \geq 0, v - h(A) = v_0 - h(A_0)\}$$

$$S_1(\mathbf{w}_0) = \left\{(A,Q); A \geq 0, v = v_0 - (A - A_0)\left[\frac{I_1(A) - I_1(A_0)}{(A-A_0)AA_0}\right]^{1/2}\right\}$$

$$S_2(\mathbf{w}_0) = \left\{(A,Q); A \geq 0, v = v_0 + (A - A_0)\left[\frac{I_1(A) - I_1(A_0)}{(A-A_0)AA_0}\right]^{1/2}\right\}.$$

$$v = \frac{Q}{A}, \;, v_0 = \frac{Q_0}{A_0} \text{ and } h(A) = \int_{A^\star}^{A} \frac{c(s)}{s} ds$$

$A^\star \geq 0$ is some arbitrary reference state.

$\Sigma_1(\mathbf{w}_0)$ represents the states $\mathbf{w}$ that can be connected to $\mathbf{w}_0$ on the right by either a 1-shock or a 1-rarefaction. $\Sigma_2(\mathbf{w}_0)$ represents the states $\mathbf{w}$ that can be connected to $\mathbf{w}_0$ on the left by either a 2-shock or a 2-rarefaction (see [13] for more details)

$$\Sigma_1(\mathbf{w}_0) = \{\mathbf{w}; A \geq 0, \mathbf{w} \in \Gamma_1(\mathbf{w}_0) \text{ if } A \leq A_0; \mathbf{w} \in S_1(\mathbf{w}_0) \text{ if } A > A_0\}$$

$$\Sigma_2(\mathbf{w}_0) = \{\mathbf{w}; A \geq 0, \mathbf{w} \in \Gamma_2(\mathbf{w}_0) \text{ if } A \leq A_0; \mathbf{w} \in S_2(\mathbf{w}_0) \text{ if } A > A_0\}$$

If we solve exactly each Riemann problem, and then calculate the cell averages at the new time level, we get the Godunov scheme

$$\mathbf{w}_j^{n+1} = \mathbf{w}_J^n - \frac{\Delta t}{\Delta x}(\mathbf{F}(\mathbf{w}_{j+1/2}^{(R)}) - \mathbf{F}(\mathbf{w}_{j-1/2}^{(R)}))$$

where $\mathbf{w}_{j+1/2}^{(R)} = \mathbf{w}^{(R)}(0, \mathbf{w}_j^n, \mathbf{w}_{j+1}^n)$.

We need the CFL condition

$$\max(|\lambda_1|, |\lambda_2|)\frac{\Delta t}{\Delta x} \leq 1$$

$$\mathbf{w}_s = \Gamma_1(\mathbf{w}_L) \cap \{\lambda_1 = 0\} \quad \text{if } \lambda_1(\mathbf{w}_L) < 0 \leq \lambda_1(\bar{\mathbf{w}}),$$

$$\mathbf{w}_s = \Gamma_2(\mathbf{w}_R) \cap \{\lambda_2 = 0\} \quad \text{if } \lambda_2(\bar{\mathbf{w}}) < 0 \leq \lambda_2(\mathbf{w}_R),$$

$$\mathbf{w}_s = \bar{\mathbf{w}} \qquad \text{in other cases.}$$

$\bar{\mathbf{w}}$ is given by the non-trivial intersection of $\Sigma_1(\mathbf{w}_L)$ and $\Sigma_2(\mathbf{w}_R)$ (see figure 5.1). This is the constant state in the solution of the Riemann problem. A non-linear equation needs to be solved, in order to calculate $\bar{\mathbf{w}}$.

The source term $\mathbf{D}$ is implemented in a pointwise manner, the same as in the Osher and Solomon scheme.

The boundary conditions are implemented by calculating an imaginary state $\mathbf{w}^\star$ next to the boundary (outside region) such that, when using the scheme on the boundary, it results in the correct value being given to A.

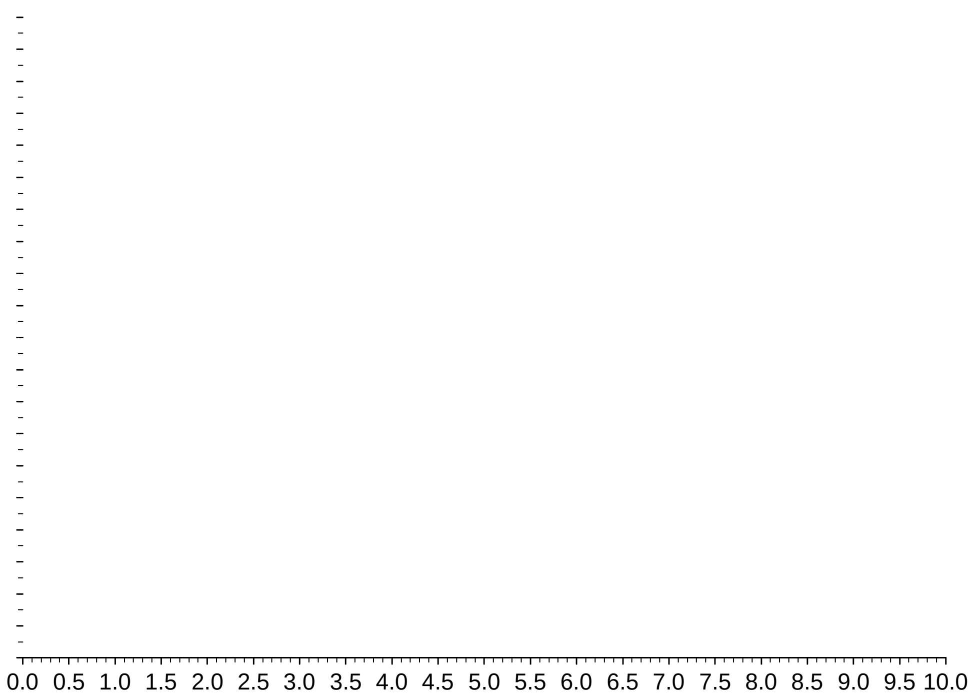
0.0 0.5 1.0 1.5 2.0 2.5 3.0 3.5 4.0 4.5 5.0 5.5 6.0 6.5 7.0 7.5 8.0 8.5 9.0 9.5 10.0

Figure 6.1 is a plot of the sets of eigenvalues, $\{\lambda_{1,j+1/2}\}, \{\lambda_{2,j+1/2}\}$ from Roe's scheme. The sharp change in the eigenvalues occurs where the flow changes from being above the soffit to below it. It was thought that these sharp jumps were the cause of the oscillations. To test this, the eigenvalues were processed, after being calculated, so as to reduce the sharpness of the jump. These new sets of eigenvalues, $\{\lambda^{\star}_{1,j+1/2}\}, \{\lambda^{\star}_{2,j+1/2}\}$, were then used in the calculation of all further quantities. The 'smoothing' process was carried out for each time step, and in the following way,

$$\lambda^{\star}_{i,j+1/2} = \lambda_{i,j+1/2} + \epsilon \Delta t \delta^2_{j+1/2} \lambda_{i,j+1/2}$$

$i = 1, 2$ and $j = 1, \ldots\ldots, N-2$, where

$$\delta^2_{j+1/2} \lambda_{i,j+1/2} = \frac{\lambda_{i,j-1/2} - 2\lambda_{i,j+1/2} + \lambda_{i,j+3/2}}{\Delta x^2}$$

and ϵ is a free parameter.

6.1.1 Results and Discussion

Figure 6.2 shows the modified eigenvalues, at the same time as in figure 6.1. These have been generated from the modified scheme, using smoothing at each time step. The value used for ϵ was 0.5. Figure 6.3 shows the corresponding time history for this modified scheme, compared to normal Roe.

There is significant improvement in the oscillations, however we have slightly modified the other properties of the solution. Notice in particular the loss in height at, and after the oscillations; this loss is not recovered later on in time. Increasing ϵ results in the oscillations being reduced in size, however, the deterioration described above increases. As we reduce ϵ the oscillations grow, and the

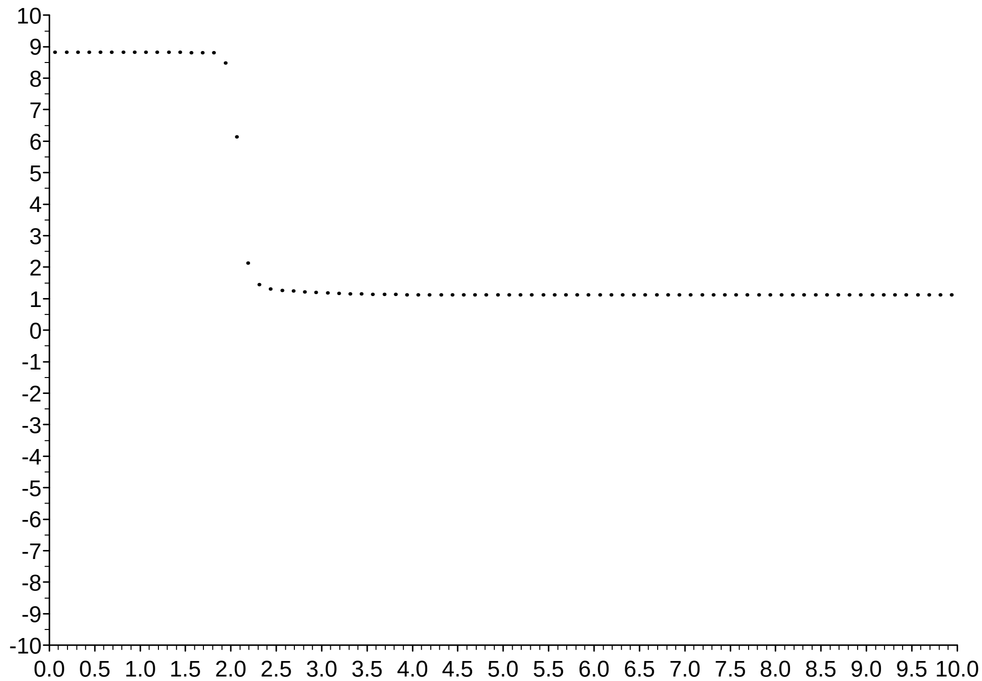
10
9
8
7
6
5
4
3
2
1
0
-1
-2
-3
-4
-5
-6
-7
-8
-9
-10
0.0 0.5 1.0 1.5 2.0 2.5 3.0 3.5 4.0 4.5 5.0 5.5 6.0 6.5 7.0 7.5 8.0 8.5 9.0 9.5 10.0

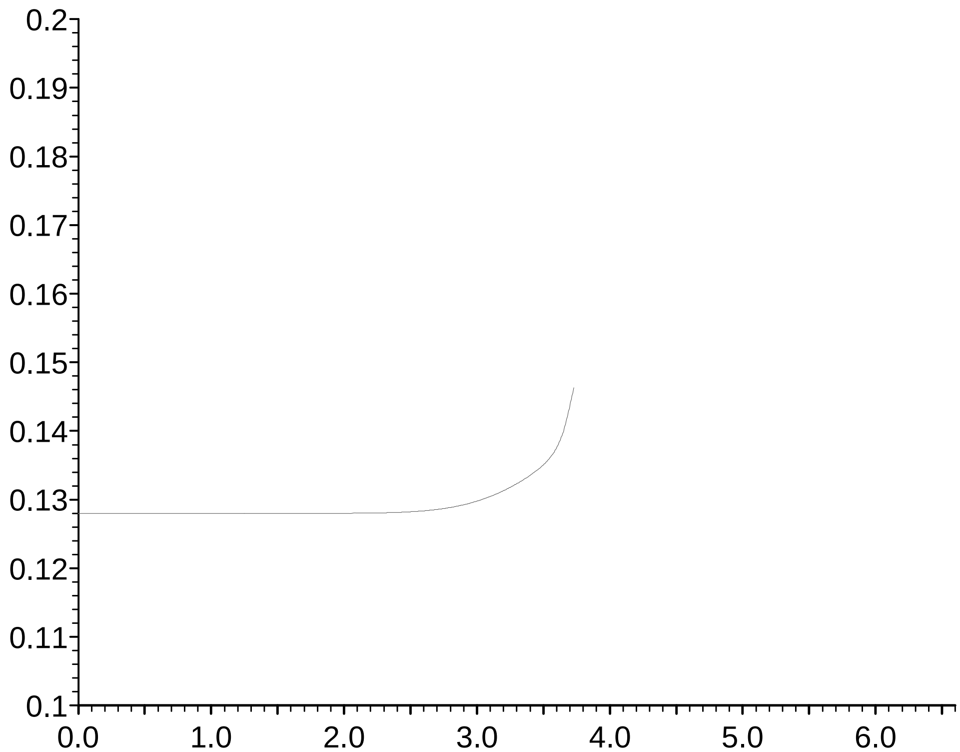
0.2
0.19
0.18
0.17
0.16
0.15
0.14
0.13
0.12
0.11
0.1
0.0
1.0
2.0
3.0
4.0
5.0
6.0

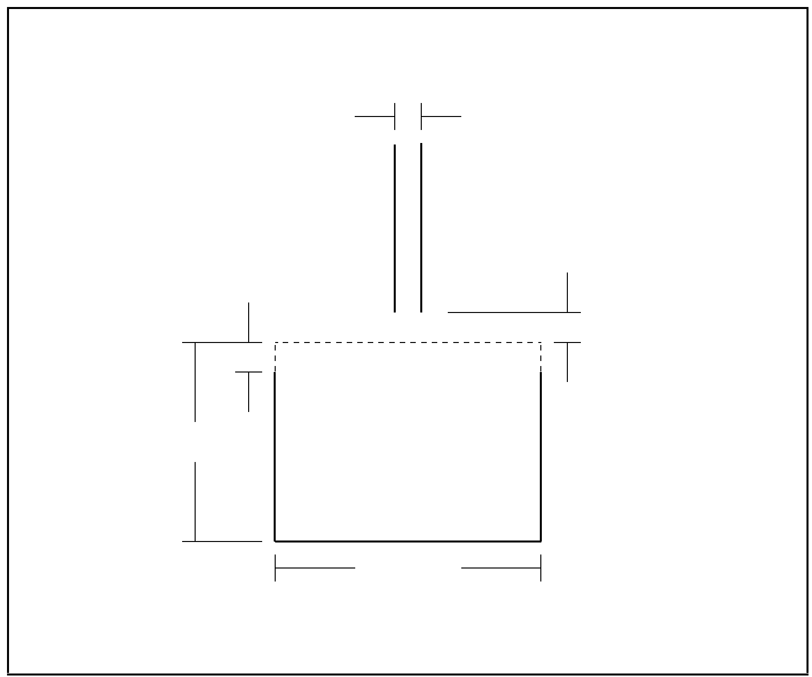

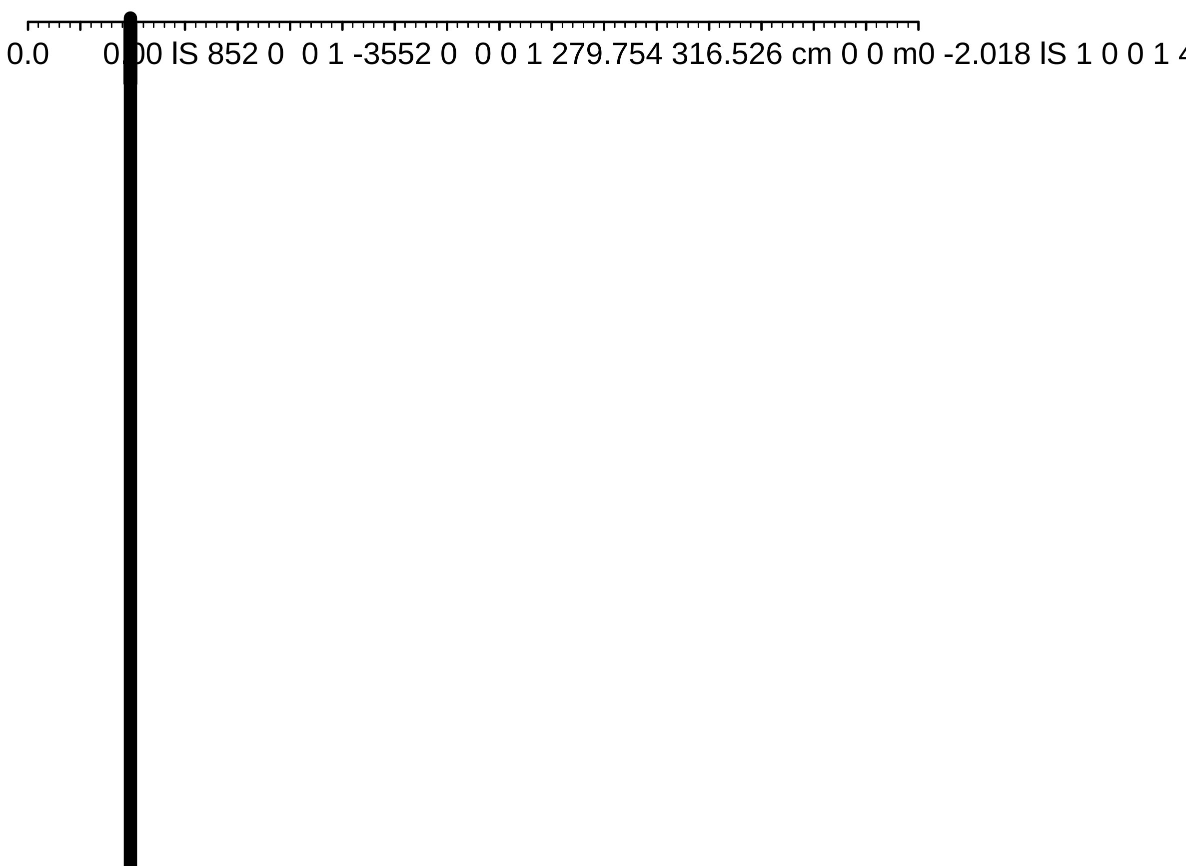
0.0
0.00 IS 852 0 0 1 -3552 0 0 0 1 279.754 316.526 cm 0 0 m0 -2.018 IS 1 0 0 1 4

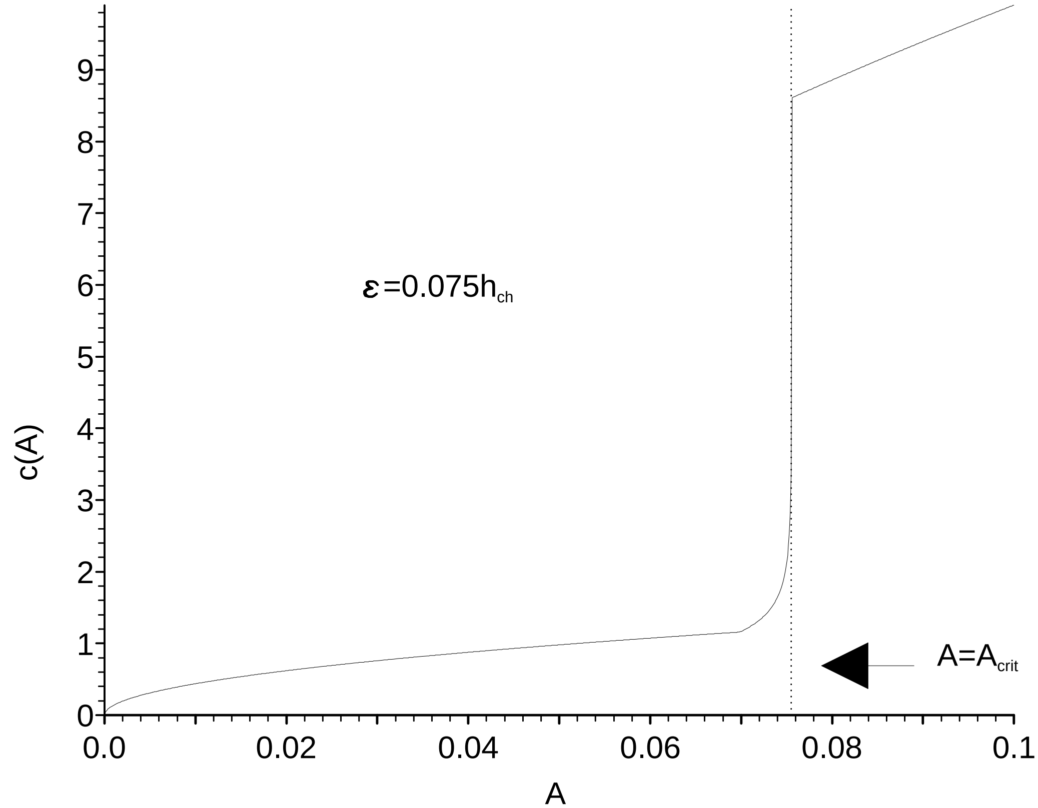

Figure 6.6: $c(A)$ for modified channel ($\epsilon = 0.075h_{ch}$).

better than when smoothing the eigenvalues, since we do not lose height after the oscillations as in that method. Figure 6.8 shows the results for $\epsilon = 0.11h_{ch}$; notice the further deterioration of the solution, but the smaller oscillations. An ϵ of about $0.075h_{ch}$ was found to give, visually, the best results.

Roe's scheme can be written in the following form

$$\frac{\mathbf{W}^{n+1} - \mathbf{W}^{n}}{\Delta t} = \mathbf{G}(\mathbf{W}^{n}) \tag{7.1}$$

where

$$\mathbf{W}^{n} = \begin{bmatrix} \mathbf{w}_0^n \\ \mathbf{w}_1^n \\ \vdots \\ \mathbf{w}_N^n \end{bmatrix}, \mathbf{G}(\mathbf{W}) = \begin{bmatrix} \mathbf{g}_0 \\ \mathbf{g}_1 \\ \vdots \\ \mathbf{g}_N \end{bmatrix}.$$

$\mathbf{g}_j$ is the Roe approximation of

$$\left. -\frac{\partial \mathbf{F}(\mathbf{w})}{\partial x} + \mathbf{D} \right|_{x=j\Delta x}$$

using the states $\mathbf{W}$. Where we mean the usual Roe approximation to the space derivative of $\mathbf{F}$ and the upwinding approximation to $\mathbf{D}$ (as in section 3.1).

7.1 Implicit Roe's Scheme

One way to make Roe's scheme implicit is in the following way,

$$\frac{\mathbf{W}^{n+1} - \mathbf{W}^{n}}{\Delta t} = \mathbf{G}(\mathbf{W}^{n+\theta})$$

where

$$\mathbf{W}^{n+\theta} = (1-\theta)\mathbf{W}^{n} + \theta\mathbf{W}^{n+1}.$$

An iterative method is needed to carry out this scheme, since $\mathbf{W}^{n+1}$ is unknown. We initially set $\mathbf{W}^{n+1} = \mathbf{W}^{n}$, then use the scheme to calculate a better approximation to $\mathbf{W}^{n+1}$; this value is then used to get a better approximation, and so on. We stop the process when we have got an accurate enough value. Of course we need to implement the boundary conditions as usual, after the iteration has converged.

Implicit schemes are well known to be more stable, than their corresponding explicit schemes. This probably contributes to a good improvement in the oscillations; see figure 7.1 for results for $\theta = 1$. There is a similar improvement as for the smoothing techniques, but in this case there is no deterioration in the solution. The implicit scheme is much more time consuming than the explicit version, and this may make it impractical. The best value for θ was found to be 1.0.

Figure 7.2 shows results from using the implicit scheme, with the modified channel ($\theta = 1, \epsilon = 0.75h_{ch}$). These are probably the best results seen so far; the oscillations are very small, and the rest of the solution compares well with Roe.

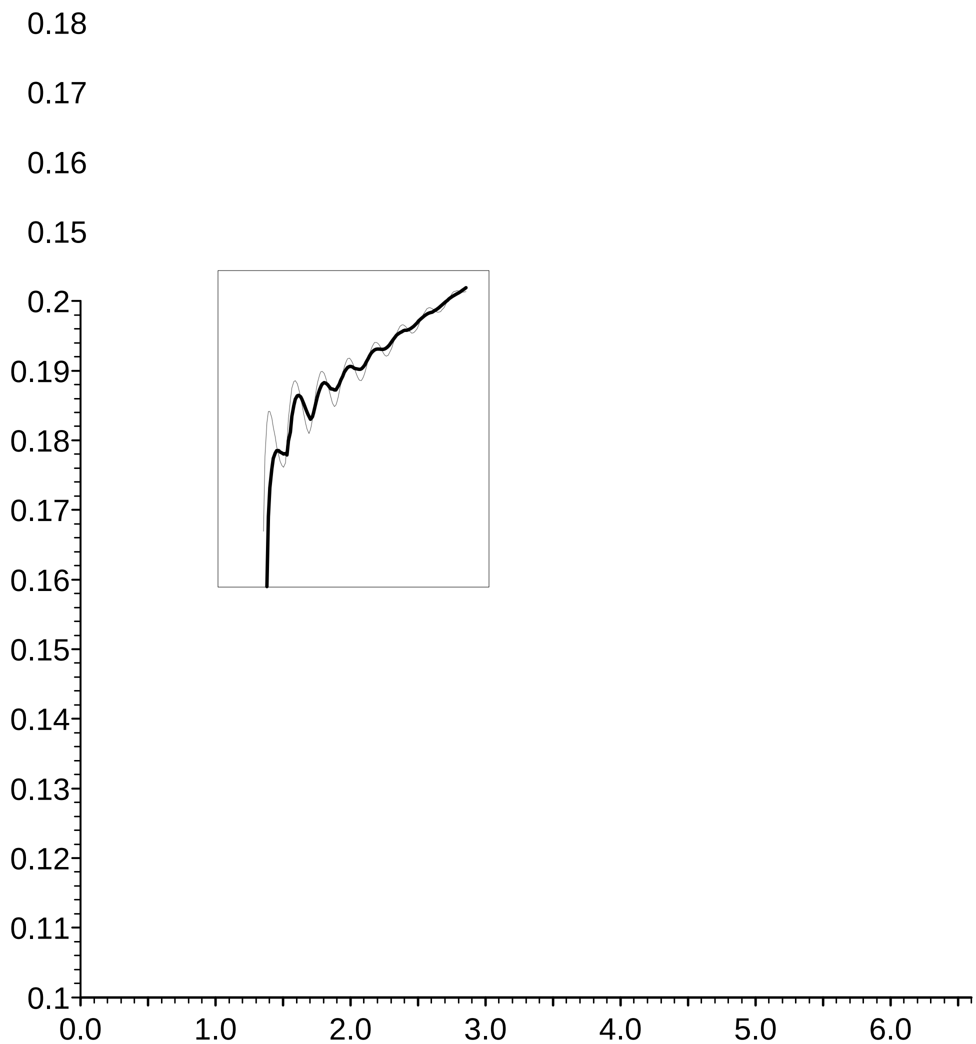
0.18
0.17
0.16
0.15
0.2
0.19
0.18
0.17
0.16
0.15
0.14
0.13
0.12
0.11
0.1
0.0
1.0
2.0
3.0
4.0
5.0
6.0

7.2 Alternative Time Stepping

From equation 7.1 it can be seen that Roe's scheme uses uler time stepping. It would be an idea to try and change to a different time stepping, in order to see what difference this would make. See [10] for more information on different time steppings. First we tried using Runge-Kutta fourth-order as follows,

$$\mathbf{W}^{n+1} = \mathbf{W}^n + \frac{\Delta t}{6}(\mathbf{K}_1 + 2\mathbf{K}_2 + 2\mathbf{K}_3 + \mathbf{K}_4)$$

where

$$\begin{aligned}
\mathbf{K}_1 &= \mathbf{G}(\mathbf{W}^n) \\
\mathbf{K}_2 &= \mathbf{G}(\mathbf{W}^n + \tfrac{\Delta t}{2}\mathbf{K}_1) \\
\mathbf{K}_3 &= \mathbf{G}(\mathbf{W}^n + \tfrac{\Delta t}{2}\mathbf{K}_2) \\
\mathbf{K}_4 &= \mathbf{G}(\mathbf{W}^n + \mathbf{K}_3).
\end{aligned}$$

The Runge-Kutta fourth-order scheme results in a slight improvement in the oscillations, but not as much as the implicit scheme in the previous section. This can be seen from the results in figure 7.3.

Linear Multistep Methods were also tried, including implicit ones; some were unstable and needed the CFL number reducing. None of these gave an improvement better than the implicit scheme described in the previous section.

Ch pter 8

Shock' Fitting

8.1 Description

There is now quite a lot of evidence indicating that the problem is due to piecewise constant states, approximating sharply varying functions. In this problem, the front at the pressurized/free surface interface is so sharp that we could treat it like a discontinuity. If we were to ensure that the front was at the interface between two grid cells, then the solution in both the neighbouring cells would be smooth; hence piece-wise constants would then be a valid approximation. In order for us to do this, we will need to work on a non-uniform grid and allow the grid to alter in time. We will also need to be able to find and keep track of the position of the front. The following is a simple way of achieving the above, by modifying Roe's scheme.

Step 1: Finding the Front.

Until the front develops, and is found, we proceed as before with the ordinary Roe's scheme. The following criterion is used to identify the front, and calculate

k k 1 k+1

1 +1

$$\frac{\quad 1}{+1}$$

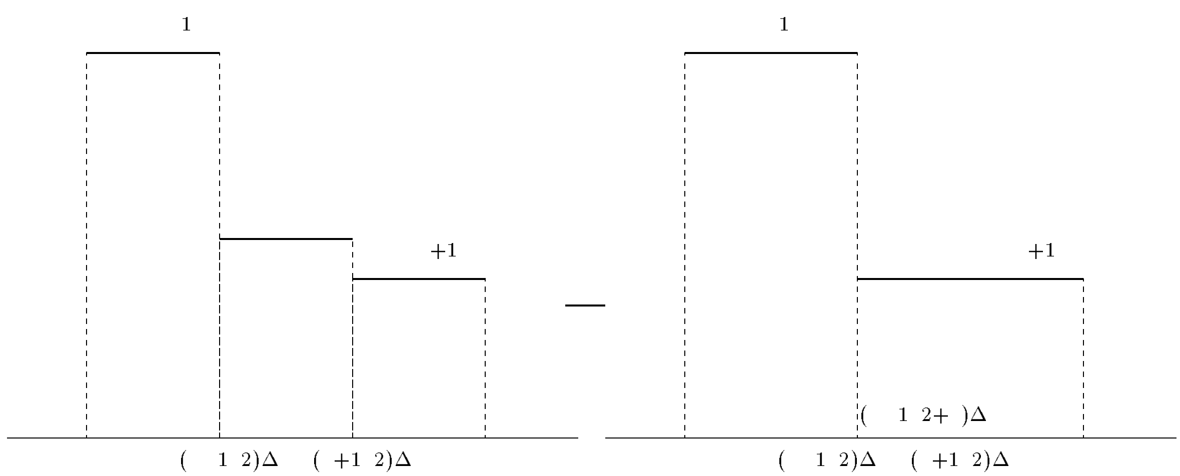

$$\frac{+1}{+1 \quad 1}$$

+1

+1 2

+1 2 +1

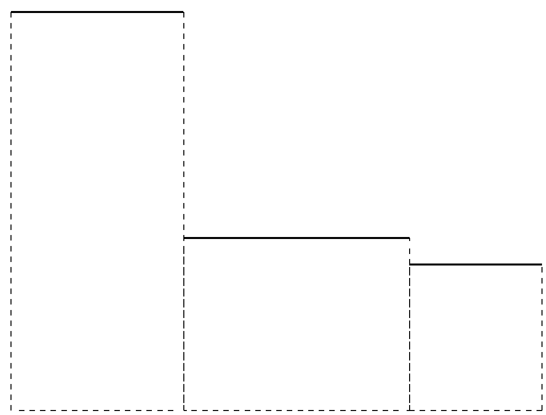

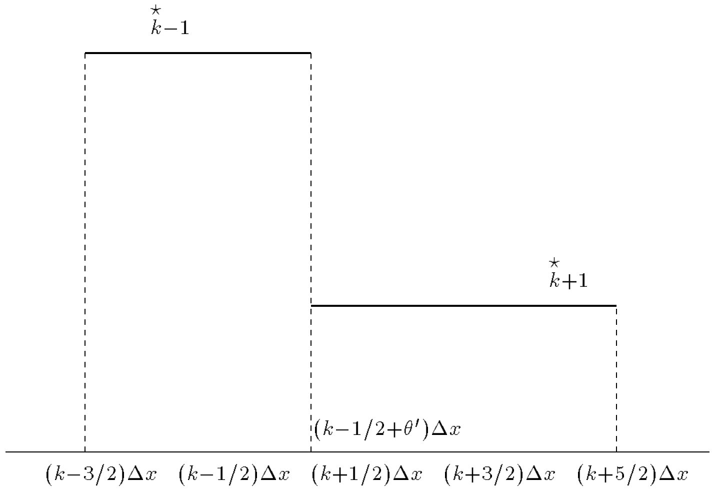

Figure 8.3: New position of discontinuity.

Recovering the original uniform states.

We now wish to get values for the original uniform grid that we started with.

$\overset{\star}{j}$

$^{n+1}_{j}$ 1

2

$\overset{\star}{j-1}$

1 2

1 2

$'$

If $\theta' \leq 1$ then the front has not moved cells. From conservation we get

$$\mathbf{z}_1 + \mathbf{z}_2 = \theta' \mathbf{w}^{\star}_{k-1} + (1-\theta')\mathbf{w}^{\star}_{k+1}.$$

The new position of the front gives

$$\theta' \mathbf{w}^{\star}_{k-1} + (1-\theta')\mathbf{z}_2 = \mathbf{z}_1.$$

We solve these two equations for $\mathbf{z}_1$ and $\mathbf{z}_2$.

If $\theta' > 1$ then the front has moved one cell to the right. From conservation we get

$$\mathbf{z}_1 + \mathbf{z}_2 = \theta' \mathbf{w}^{\star}_{k-1} + (1-\theta')\mathbf{w}^{\star}_{k+1}.$$

The new position of the front gives

$$(\theta' - 1)\mathbf{z}_1 + (2-\theta')\mathbf{w}^{\star}_{k+1} = \mathbf{z}_2.$$

We solve these two equations for $\mathbf{z}_1$ and $\mathbf{z}_2$.

We are now in the position to do another time step. We now know the new position of the front, so we need never repeat step 1 again; we can just start with step 2.

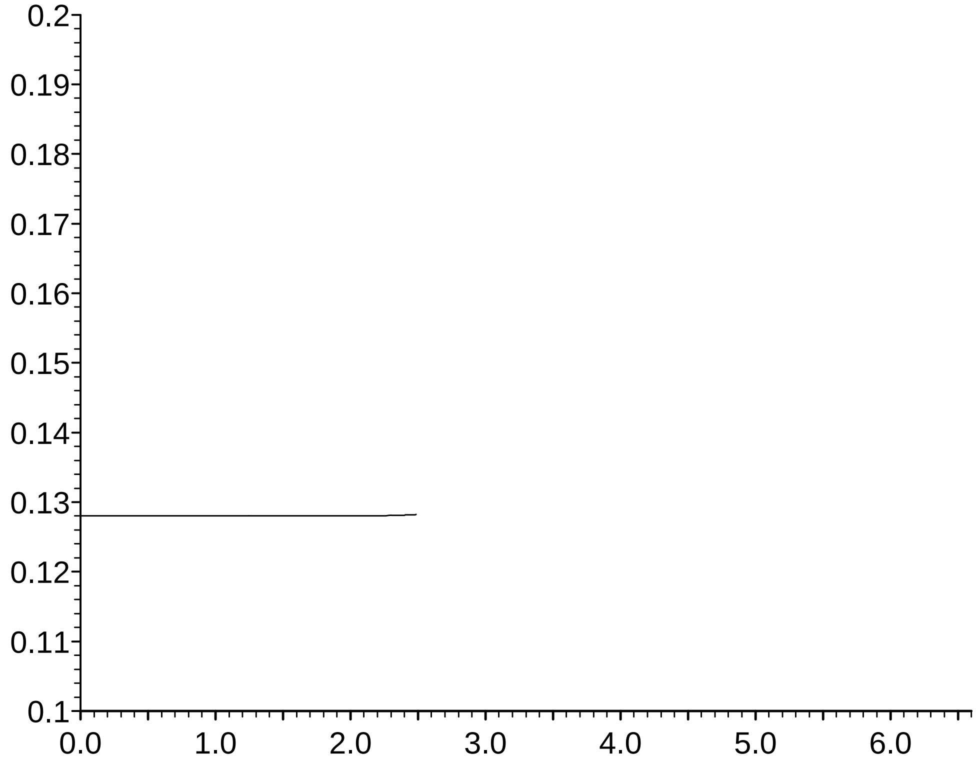
0.2
0.19
0.18
0.17
0.16
0.15
0.14
0.13
0.12
0.11
0.1
0.0
1.0
2.0
3.0
4.0
5.0
6.0

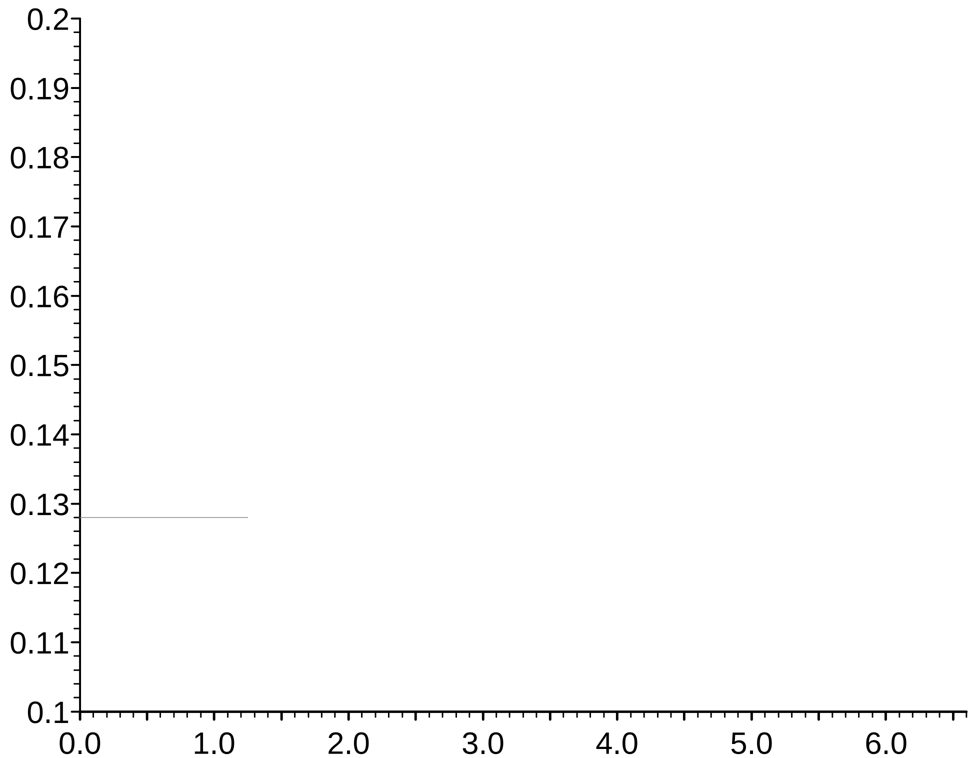

0.2
0.19
0.18
0.17
0.16
0.15
0.14
0.13
0.12
0.11
0.1
0.0
1.0
2.0
3.0
4.0
5.0
6.0

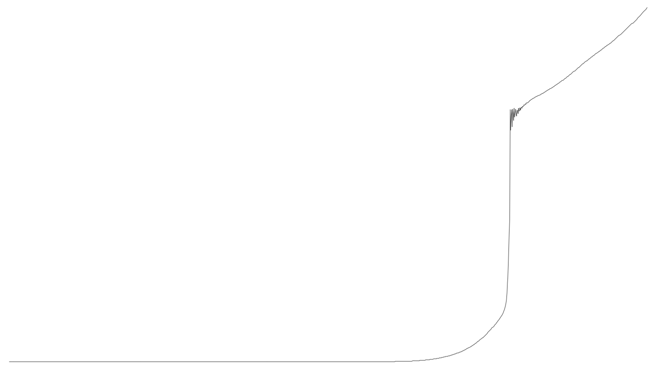

Throughout this work, we have been unable to pinpoint, exactly, the cause of the oscillations; however it is felt that we have gone some way to understanding the cause.

In chapter 5 it was concluded that the approximate nature of the Riemann solvers was not a significant factor in causing the oscillations. The approximation of piecewise constant states seemed to play a much bigger part. The first significant improvement in the oscillations was found with the smoothing techniques, however these are seriously limited by the deterioration of the solution. The implicit scheme from section 7.1 did not cause such deterioration, but was very fruitful direction. Another approach that might be considered is increasing the order of approximation, eg. using piecewise linears.

[1] , Unsteady 1-D Flows with

[7] , Upwind Difference Schemes for Hyperbolic Systems of Conservation Laws. Mathematics of Computation. v. 38, 1982, pp. 339-374.